C-Peptide Activates AMPKα and Prevents ROS-Mediated Mitochondrial Fission and Endothelial Apoptosis in Diabetes

Mahendra Prasad Bhatt, Young-Cheol Lim, Young-Myeong Kim, and Kwon-Soo Ha

Vasculopathy is a major complication of diabetes; however, molecular mechanisms mediating the development of vasculopathy and potential strategies for prevention have not been identified. We have previously reported that C-peptide prevents diabetic vasculopathy by inhibiting reactive oxygen species (ROS)-mediated endothelial apoptosis. To gain further insight into ROS-dependent mechanism of diabetic vasculopathy and its prevention, we studied high glucose–induced cytosolic and mitochondrial ROS production and its effect on altered mitochondrial dynamics and apoptosis. For the therapeutic strategy, we investigated the vasoprotective mechanism of C-peptide against hyperglycemia-induced endothelial damage through the AMP-activated protein kinase α (AMPKα) pathway using human umbilical vein endothelial cells and aorta of diabetic mice. High glucose (33 mmol/L) increased intracellular ROS through a mechanism involving interregulation between cytosolic and mitochondrial ROS generation. C-peptide (1 nmol/L) activation of AMPKα inhibited high glucose–induced ROS generation, mitochondrial fission, mitochondrial membrane potential collapse, and endothelial cell apoptosis. Additionally, the AMPK activator 5-aminoimidazole-4-carboxamide 1-β-D-ribofuranoside and the antihyperglycemic drug metformin mimicked protective effects of C-peptide. C-peptide replacement therapy normalized hyperglycemia-induced AMPKα dephosphorylation, ROS generation, and mitochondrial disorganization in aorta of diabetic mice. These findings highlight a novel mechanism by which C-peptide activates AMPKα and protects against hyperglycemia-induced vasculopathy. ***Diabetes* 62:3851–3862, 2013**

C-peptide and insulin are cosecreted in equimolar amounts into the circulation from the pancreatic β-cells of Langerhans (1). C-peptide deficiency is a prominent attribute of type 1 diabetes (1). Deficiencies of C-peptide and insulin may also occur in the late stages of type 2 diabetes as a result of progressive loss of β-cells (2–4). Recent evidence demonstrates a beneficial role for C-peptide in diabetic neuropathy (1,5,6), nephropathy (1,6,7), and vascular dysfunction (1,5) and inflammation (1). C-peptide protects against diabetic vascular damage by promoting nitric oxide (NO) release (8) and suppressing nuclear factor-κB (9), which suppresses leukocyte-endothelium interactions (8,9). C-peptide may prevent atherosclerosis by inhibiting vascular smooth muscle proliferation and migration (10) and reducing venous neointima formation (11). However, the molecular mechanism by which C-peptide prevents diabetes complications is not understood well enough to permit its clinical implementation.

Generation of reactive oxygen species (ROS) in response to high glucose is the leading cause of endothelial damage and diabetic vasculopathy (12). Protein kinase C (PKC)-dependent NADPH oxidase is considered a major cytosolic mediator of ROS generation in endothelial cells (13,14) that play a central role in hyperglycemia-induced endothelial cell apoptosis and vascular complications (15–17). Overproduction of intracellular ROS by mitochondria also occurs during the development of hyperglycemia-induced vascular complications (12,18,19). Altered mitochondrial dynamics due to mitochondrial fission were recently linked with endothelial dysfunction in diabetes (20,21). However, the mechanisms regulating production of cytosolic and mitochondrial ROS and their individual functions in regulating mitochondrial dynamics and apoptosis remain to be elucidated.

AMP-activated protein kinase (AMPK) is an intracellular energy and stress sensor (22) and is an emerging target for preventing diabetes complications (23), as exhibited by the most common antihyperglycemic drugs, rosiglitazone (24) and metformin (25). AMPK prevents apoptosis of endothelial cells (26–28) by inhibiting ROS generation by NADPH oxidase (24,29) and mitochondria (30). Additionally, AMPK dephosphorylation is associated with diabetes (22,31,32). It has been reported that C-peptide inhibits high glucose–induced mitochondrial superoxide generation in renal microvascular endothelial cells (7). We recently demonstrated a key role for C-peptide in preventing high glucose–induced ROS generation and apoptosis of endothelial cells through inhibition of transglutaminase (17). However, the mechanism underlying C-peptide–mediated inhibition of intracellular ROS production and subsequent apoptosis remains unclear. Thus, we hypothesized that the potential protective role of C-peptide could be attributed to activation of AMPK, which results in reduced hyperglycemia-induced production of intracellular ROS and altered mitochondrial dynamics that suppress apoptosis of endothelial cells.

In this study, we sought to elucidate the mechanism by which C-peptide protects against hyperglycemia-induced ROS production and subsequent endothelial cell damage. We examined the beneficial effect of C-peptide through AMPKα activation and subsequent protection against hyperglycemia-induced production of intracellular ROS, dysregulation of mitochondrial dynamics, mitochondrial membrane potential ($\Delta\Psi_m$) collapse, and apoptosis of endothelial cells. These studies were confirmed in vivo in mice with streptozotocin-induced diabetes using C-peptide supplement therapy delivered through osmotic pumps.

From the Department of Molecular and Cellular Biochemistry, Kangwon National University School of Medicine, Chuncheon, Korea.
Corresponding author: Kwon-Soo Ha, ksha@kangwon.ac.kr.
Received 10 January 2013 and accepted 17 July 2013.
DOI: 10.2337/db13-0039
This article contains Supplementary Data online at http://diabetes.diabetesjournals.org/lookup/suppl/doi:10.2337/db13-0039/-/DC1.

Thus, our study implicates C-peptide replacement therapy as a potentially significant approach for preventing diabetes complications.

RESEARCH DESIGN AND METHODS

Cell culture. Human umbilical vein endothelial cells (HUVECs) were isolated from human umbilical cord veins as previously described (17). Cells were maintained in M199 culture media supplemented with 20% FBS, 3 ng/mL basic fibroblast growth factor, 5 units/mL heparin, 100 IU/mL penicillin, and 100 μg/mL streptomycin. Cells between passages 3 and 7 were incubated overnight in low-serum medium (M199 supplemented as described above except with 5% FBS, 1 ng/mL basic fibroblast growth factor, and 25 mmol/L HEPES).

Measurement of intracellular and mitochondrial ROS generation and intracellular NO production. Intracellular ROS generation was measured using H_2DCFDA staining (Molecular Probes, Eugene, OR) as previously described (17). Cells on 2% gelatin-coated coverslips were treated with 33 mmol/L D-glucose for 48 h and stained with 10 μmol/L H_2DCFDA for 10 min in serum-free, phenol red-free media. For measurement of mitochondrial ROS, cells were incubated with 5 μmol/L MitoSox Red (Molecular Probes) for 30 min in low-serum media. Cells were stained with 2 μmol/L DAF-FM diacetate (Molecular Probes) for 30 min in low-serum medium for measuring intracellular NO production. Labeled cells were immediately analyzed by confocal microscopy (Fluoview-300; Olympus). Single-cell fluorescence intensities were determined for 30 cells per experiment. The levels of intracellular and mitochondrial ROS and intracellular NO were determined by comparing fold change in fluorescence intensity of treated cells versus control cells.

Mitochondrial staining and analysis of mitochondrial fission. Cells were incubated with 33 mmol/L D-glucose for 48 h, and entire mitochondria were visualized in live cells by staining with 200 nmol/L Mito Tracker Red CMXRos (Molecular Probes) for 30 min at 37°C. Cells with a predominantly intact network of tubular mitochondria were identified as normal. Cells with disrupted and predominantly spherical mitochondria were identified as having mitochondrial fission. Ninety cells from three independent experiments were used to calculate the percentage of cells undergoing mitochondrial fission.

Measurement of $\Delta\Psi_m$. $\Delta\Psi_m$ was monitored by confocal microscopy as previously described (33). Cells were incubated with 33 mmol/L D-glucose for 48 h and stained with 2 μmol/L of JC-1 (Molecular Probes) for 30 min at 37°C. Fluorescence intensities were determined at the single-cell level using confocal microscopy. Data are expressed as a normalized ratio of the fluorescence intensity of the monomeric form (green) to the J-aggregate form (red).

Measurement of apoptosis. Cell death was assessed by 3,3′-dihexyloxacarbocyanine iodide ($DiOC_6$)/propidium iodide (PI) double staining using confocal microscopy as previously described (34). Briefly, cells were incubated with 33 mmol/L D-glucose for 72 h and stained with 50 nmol/L $DiOC_6$ and 10 μg/mL PI for 20 min. Stained cells were analyzed by confocal microscopy and differentiated as viable cells ($DiOC_6^{bright}/PI^-$), early apoptotic cells ($DiOC_6^{dim}/PI^-$), and late apoptotic cells ($DiOC_6^{dim}/PI^+$). Total cell death (defined as the sum of early and late apoptotic cells) and frequency distributions were expressed as percentages of the total cell number.

Transfection of small interfering RNA. To suppress AMPKα expression, HUVECs were transfected with AMPKα1/2-specific small interfering (si)RNA (Santa Cruz Biotechnology, Santa Cruz, CA) according to the manufacturer's instructions. Briefly, subconfluent cells were transfected overnight with the AMPKα siRNA duplex, which was synthesized to target the coding sequence of human AMPKα1/2 mRNA. A noncoding siRNA (Dharmacon, Lafayette, CO) was used as a control. Transfection was performed using siLentFect Lipid Reagent (Bio-Rad Laboratories, Hercules, CA) for 24 h.

Generation of diabetes mouse model and C-peptide replacement therapy using osmotic pumps. Six-week old male C57BL/6 mice were obtained from KOTECH (Pyungtaek, Korea). Experiments were performed in accordance with the guidelines of the Kangwon Institutional Animal Care and Use Ethics Committee. Diabetes was induced in mice by a single injection of streptozotocin (150 mg/kg body wt i.p.) as previously described (17). Sufficient hyperglycemia was observed 2 days postinjection as determined by measuring blood glucose and glucosuria. Mice with nonfasting blood glucose levels >16 mmol/L, polyuria, and glucosuria were considered diabetic. One week after the streptozotocin injection, an Alzet mini-osmotic pump 2004 (DURECT, Cupertino, CA) containing C-peptide (American Peptide Company, Sunnyvale, CA) in PBS with a delivery rate of 35 pmol/min/kg was subcutaneously implanted into each diabetic mouse in one group. The other diabetic and control mice received sham operations. During the continuous subcutaneous C-peptide perfusion, serum C-peptide levels were measured using a C-peptide Enzyme Immunoassay Kit (RayBiotech, Norcross, GA). During the whole course of these experiments, the vital statistics of each mouse were recorded.

Measurement of ROS generation and mitochondrial fission in aortic endothelium of mice. Aorta from control (n = 8), diabetic (n = 8), and C-peptide–supplemented diabetic (n = 7) mice were dissected and cut longitudinally to open the endothelium for immediate staining. For intracellular ROS measurements, aortic segments were quickly transferred to serum-free M199 media and incubated at 37°C with H_2DCFDA for 10 min. For assessment of mitochondrial fission, endothelial layers from each group were stained at 37°C for 30 min with 200 nmol/L MitoTracker Red CMXRos. Stained aortic segments were mounted on glass slides and quickly observed by confocal microscopy.

Western blot analysis. Proteins were extracted from HUVECs and aortic segments of mice with lysis buffer containing 50 mmol/L HEPES (pH 7.5), 1 mmol/L EDTA, 150 mmol/L sodium chloride, 1% Triton X-100, 10 μg/mL aprotinin, 10 μg/mL leupeptin, 0.1 mmol/L phenylmethanesulfonylfluoride, 25 mmol/L β-glycerophosphate, and 2 mmol/L sodium orthovanadate. Protein extracts were resolved by SDS-PAGE and transferred to polyvinylidene difluoride membranes. Protein expression was analyzed with monoclonal antibodies against phospho-AMPKα, AMPKα, dynamin-related protein 1 (Drp-1) (Cell Signaling Technology, Beverly, MA), and fission-1 protein (Fis-1) (Santa Cruz Biotechnology). Protein bands were visualized with a chemiluminescence reagent (Pierce, Rockford, IL).

Statistical analyses. Data processing was performed using Origin 6.1 (OriginLab, Northampton, MA) and expressed as mean ± SD of at least three independent experiments. Statistical significance was determined using ANOVA. A value of $P < 0.05$ was considered statistically significant.

RESULTS

High glucose–induced generation of cytosolic ROS facilitates mitochondrial ROS production. In HUVECs, high glucose (33 mmol/L) significantly increased the levels of intracellular and mitochondrial ROS (Fig. 1*A* and *B*). However, osmotic control L-glucose had no effect on the ROS levels (Fig. 1*B*). To understand the effect of cytosolic ROS on mitochondrial ROS levels, we inhibited PKC and NADPH oxidase that mediate high glucose–induced cytosolic ROS generation in endothelial cells. The PKC inhibitors, GF109203X and Ro-31-8220, attenuated high glucose–induced generation of intracellular and mitochondrial ROS in a dose-dependent manner (Fig. 1*C*). The well-established NADPH oxidase inhibitors, apocynin and diphenyliodinium (DPI), also prevented intracellular and mitochondrial ROS production in a dose-dependent manner (Fig. 1*D*). These results suggest that PKC-dependent activation of NADPH oxidase increases cytosolic ROS, which then promotes mitochondrial ROS generation under hyperglycemic conditions.

High glucose–induced mitochondrial ROS generation regulates increased intracellular ROS. The superoxide dismutase 2 mimetic Mito-TEMPO inhibited high glucose–induced mitochondrial ROS levels in a dose-dependent manner (Fig. 1*E*). Interestingly, high glucose–induced intracellular ROS was also inhibited by mito-TEMPO in a dose-dependent manner at a rate similar to mitochondrial ROS inhibition (Fig. 1*E*). The role of mitochondrial ROS in the regulation of intracellular ROS was further investigated using Mdivi-1, a potent inhibitor of Drp-1–mediated mitochondrial fission (35). Mitochondrial fission is believed to be an important cause of hyperglycemia-induced endothelial damage as a result of overproduction of mitochondrial ROS (20). Mdivi-1 inhibited high glucose–induced production of mitochondrial and intracellular ROS in a dose-dependent manner (Fig. 1*F*). Thus, mitochondrial ROS regulates production of intracellular ROS in response to high glucose. Blocking the production of cytosolic ROS inhibits mitochondrial ROS generation, demonstrating a potential interregulation between cytosolic and mitochondrial ROS in response to high glucose in endothelial cells.

Both cytosolic and mitochondrial ROS mediate high glucose–induced mitochondrial fission and $\Delta\Psi_m$ collapse. High-glucose treatment significantly induced mitochondrial fission in HUVECs as assessed by MitoTracker Red staining. Control cells showed an intact mitochondrial network. Cells bearing predominantly fragmented and spherical mitochondria were considered to have undergone mitochondrial fission (Fig. 2*A* and *B*). High glucose–induced mitochondrial fission was prevented by PKC inhibitors GF109203X and Ro-31-8220 and NADPH oxidase inhibitors apocynin and DPI (Fig. 2*C*). These inhibitors also blocked cytosolic ROS generation in response to high glucose in endothelial cells (Fig. 1*C* and *D*). However, L-glucose had no effect on mitochondrial fission (Fig. 2*B*). High glucose–induced mitochondrial fission was also normalized using mito-TEMPO and Mdivi-1 (Fig. 2*D*). Thus, high glucose–induced mitochondrial fission is mediated by both cytosolic and mitochondrial ROS in endothelial cells.

High glucose stimulated $\Delta\Psi_m$ collapse in endothelial cells as assessed by JC-1 staining (Fig. 2*E*), whereas L-glucose had no effect (Fig. 2*F*). The PKC inhibitors, GF109203X and Ro-31-8220, and the NADPH oxidase inhibitors, apocynin and DPI, rescued high glucose–induced $\Delta\Psi_m$ collapse (Fig. 2*F*). Furthermore, high glucose–induced $\Delta\Psi_m$ collapse was normalized by mito-TEMPO and Mdivi-1 (Fig. 2*G*). These results demonstrate that high glucose–induced $\Delta\Psi_m$ collapse is mediated by cytosolic and mitochondrial ROS in endothelial cells.

C-peptide inhibits high glucose–induced ROS generation, mitochondrial fission, and $\Delta\Psi_m$ collapse. C-peptide inhibited high glucose–induced generation of intracellular and mitochondrial ROS in a dose-dependent manner, with maximal effect at 1 nmol/L (Fig. 3*A*). As intracellular and mitochondrial ROS both mediate high glucose–induced mitochondrial fission and $\Delta\Psi_m$ collapse (Fig. 2), we studied the effects of C-peptide on mitochondrial fission and $\Delta\Psi_m$ collapse in response to high glucose. C-peptide prevented high glucose–stimulated mitochondrial fission (Fig. 3*B*). Consistently, high glucose–induced expression of fission proteins Drp-1 and Fis-1 was inhibited by C-peptide

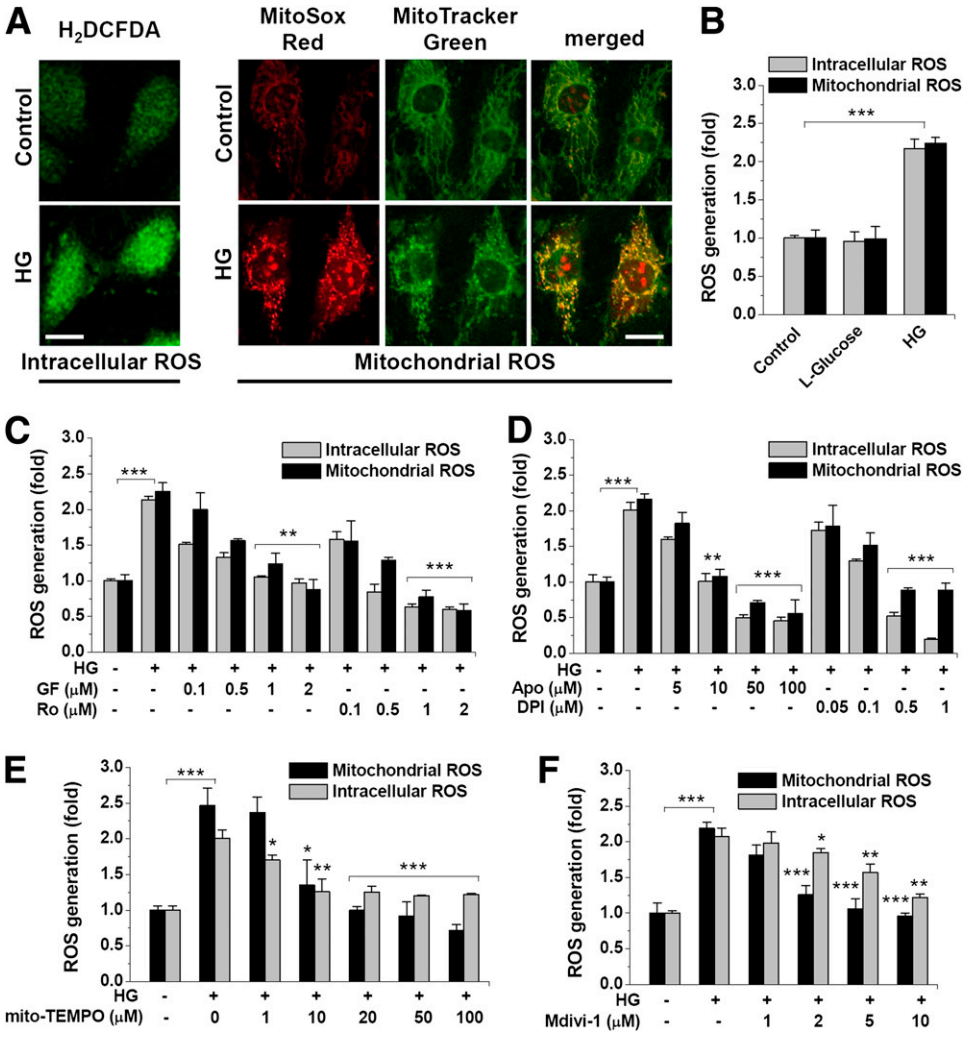

FIG. 1. Interregulation of high glucose (HG)–induced generation of intracellular and mitochondrial ROS. HUVECs were incubated for 48 h (h) with HG (33 mmol/L D-glucose) in the presence of inhibitors at the indicated concentrations. Intracellular and mitochondrial ROS levels were determined by confocal microscopy as described in RESEARCH DESIGN AND METHODS. *A* and *B*: HG-induced increases in intracellular and mitochondrial ROS. *A*: Measurement of intracellular and mitochondrial ROS levels using H_2DCFDA (green) and MitoSox Red (red). MitoSox Red is colocalized with MitoTracker Green. Scale bar, 20 μm. *B*: HG-induced generation of intracellular and mitochondrial ROS, but L-glucose had no effect; ***$P <$ 0.001. *C–F*: Dose-dependent inhibition of HG-induced generation of intracellular and mitochondrial ROS by PKC inhibitors GF109203X (GF) and Ro-31-2880 (Ro) (*C*), NADPH oxidase inhibitors apocynin (Apo) and DPI (*D*), mito-TEMPO (*E*), and Mdivi-1 (*F*). *$P < 0.05$, **$P < 0.01$, ***$P <$ 0.001 compared with HG. Data are expressed as mean ± SD from three independent experiments.

(Fig. 3*C–E*). Additionally, C-peptide rescued high glucose–induced $\Delta\Psi_m$ collapse (Fig. 3*F*). However, heat-inactivated C-peptide had no inhibitory effect on high glucose–induced generation of intracellular and mitochondrial ROS (Fig. 3*A*), mitochondrial fission (Fig. 3*B*), or $\Delta\Psi_m$ collapse (Fig. 3*F*). Thus, C-peptide prevents high glucose–induced mitochondrial fission and $\Delta\Psi_m$ collapse by inhibiting ROS generation.

Essential roles of AMPKα in C-peptide–mediated prevention of high glucose–induced ROS generation, mitochondrial fission, and $\Delta\Psi_m$ collapse. C-peptide stimulated phosphorylation of AMPKα and reversed high glucose–induced dephosphorylation of AMPKα (Fig. 4*A* and *B*). However, heat-inactivated C-peptide had no significant effect on AMPKα phosphorylation (data not shown). AMPKα1/2-specific siRNA suppressed AMPKα expression in a dose-dependent manner (Fig. 4*C*). AMPKα knockdown reversed C-peptide–mediated inhibition of high glucose–induced intracellular and mitochondrial ROS production (Fig. 4*D*). Furthermore, the AMPK inhibitor, compound C, dose-dependently reversed C-peptide–mediated prevention of high glucose–stimulated ROS generation (Fig. 4*E*). AMPK functions as a physiological suppressor of NADPH oxidase and ROS production in endothelial

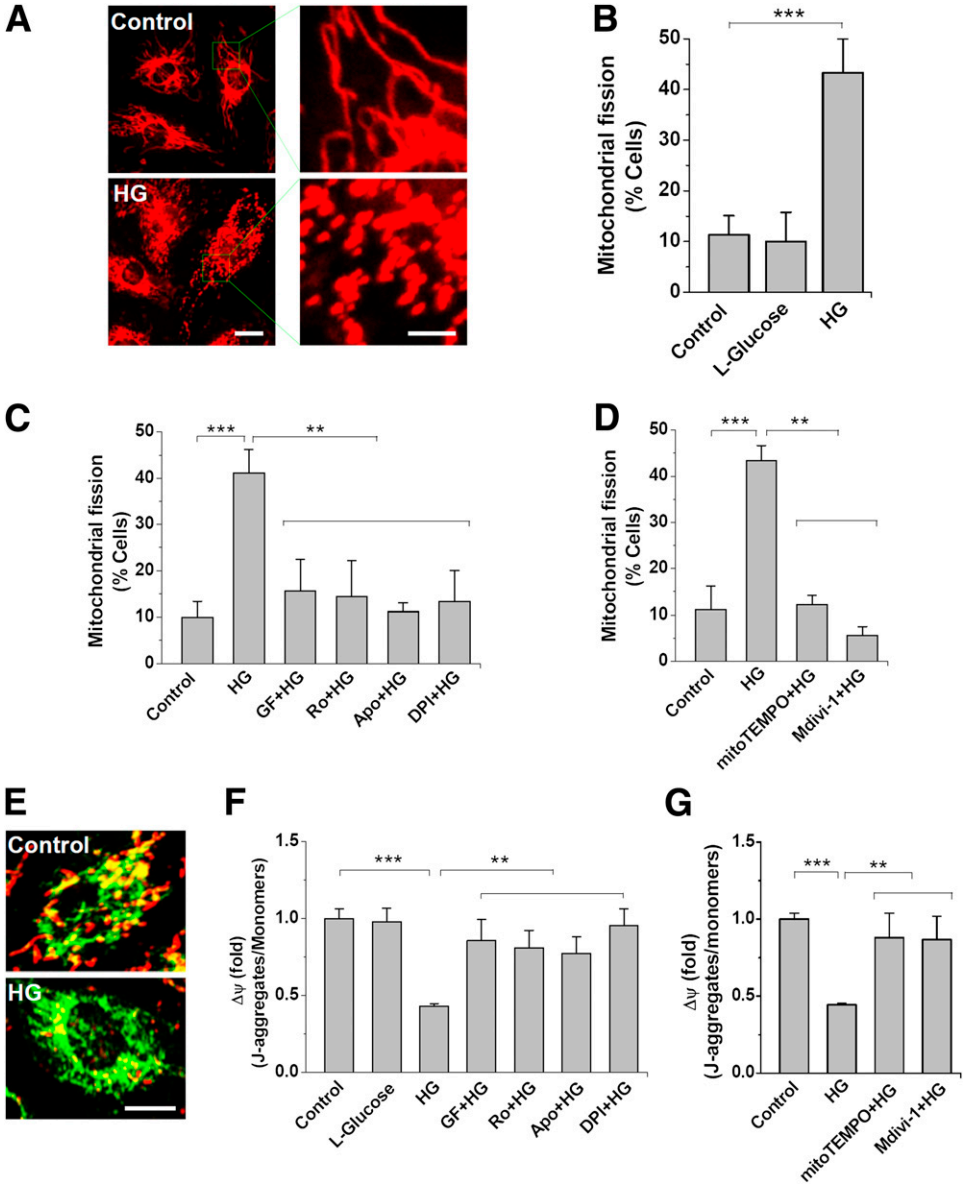

FIG. 2. Essential roles of cytosolic and mitochondrial ROS in high glucose (HG)–induced mitochondrial fission and $\Delta\Psi_m$ collapse. HUVECs were incubated with HG in the presence of inhibitors for 48 h. Mitochondrial fission and $\Delta\Psi_m$ were determined by confocal microscopy as described in RESEARCH DESIGN AND METHODS. *A*: Mitochondrial fission was represented by predominantly fragmented mitochondria in HG–exposed cells in comparison with control cells. *Left*, scale bar 20 μm; *right*, magnified images, scale bar 5 μm. *B*: Percentage of cells undergoing HG–induced mitochondrial fission. There is no effect with L-glucose. *C*: Inhibition of HG–induced mitochondrial fission by PKC inhibitors GF109203X (GF) and Ro-31-2880 (Ro) and NADPH oxidase inhibitors apocynin (Apo) and DPI. *D*: Inhibition of HG-induced mitochondrial fission by mito-TEMPO and Mdivi-1. *E*: Determination of HG–induced $\Delta\Psi_m$ collapse; scale bar 20 μm. *F*: Inhibition of HG–induced $\Delta\Psi_m$ collapse by PKC inhibitors GF109203X and Ro-31-2880 and NADPH oxidase inhibitors apocynin and DPI. However, L-glucose had no effect on $\Delta\Psi_m$ collapse. *G*: Inhibition of HG–induced $\Delta\Psi_m$ collapse by mito-TEMPO and Mdivi-1. ***$P < 0.001$, **$P < 0.01$. Data are expressed as mean ± SD of three independent experiments.

cells (29,30). Thus, it is likely that AMPKα-mediated inhibition of NADPH oxidase is an important mechanism by which C-peptide prevents production of intracellular and mitochondrial ROS in response to high glucose.

We then used AMPKα1/2 siRNA and compound C to investigate the contribution of AMPK to the altered mitochondrial dynamics stimulated by high glucose. AMPKα1/2 siRNA reversed C-peptide–mediated inhibition of mitochondrial fission in the presence of high glucose (Fig. 4*F*). Similarly, compound C prevented C-peptide–mediated inhibition of high glucose–induced mitochondrial fission (Fig. 4*G*). The essential role of AMPKα in C-peptide–mediated prevention of $\Delta\Psi_m$ collapse induced by high glucose was also found using AMPKα1/2 siRNA and compound C (Fig. 4*H* and *I*). Taken together, C-peptide inhibits high glucose–induced generation of intracellular and mitochondrial ROS through activation of AMPKα, resulting in prevention of mitochondrial fission and $\Delta\Psi_m$ collapse in endothelial cells.

Additionally, we further investigated whether NO production by C-peptide acts upstream of AMPK. C-peptide significantly elevated the level of intracellular NO at 0.5 h, with maximal effect at 2 h (Fig. 4*J*), and the elevated level returned back to the basal level at 12 h (data not shown). L-N^G-nitro-L-arginine methyl ester (L-NAME) prevented C-peptide–induced NO production, but compound C had no effect (Fig. 4*J*). C-peptide activation of AMPKα was blocked by L-NAME, and the NO donor *S*-nitroso-*N*-acetylpenicillamine reversed high glucose–induced AMPKα dephosphorylation at 48 h (Fig. 4*K* and *L*).

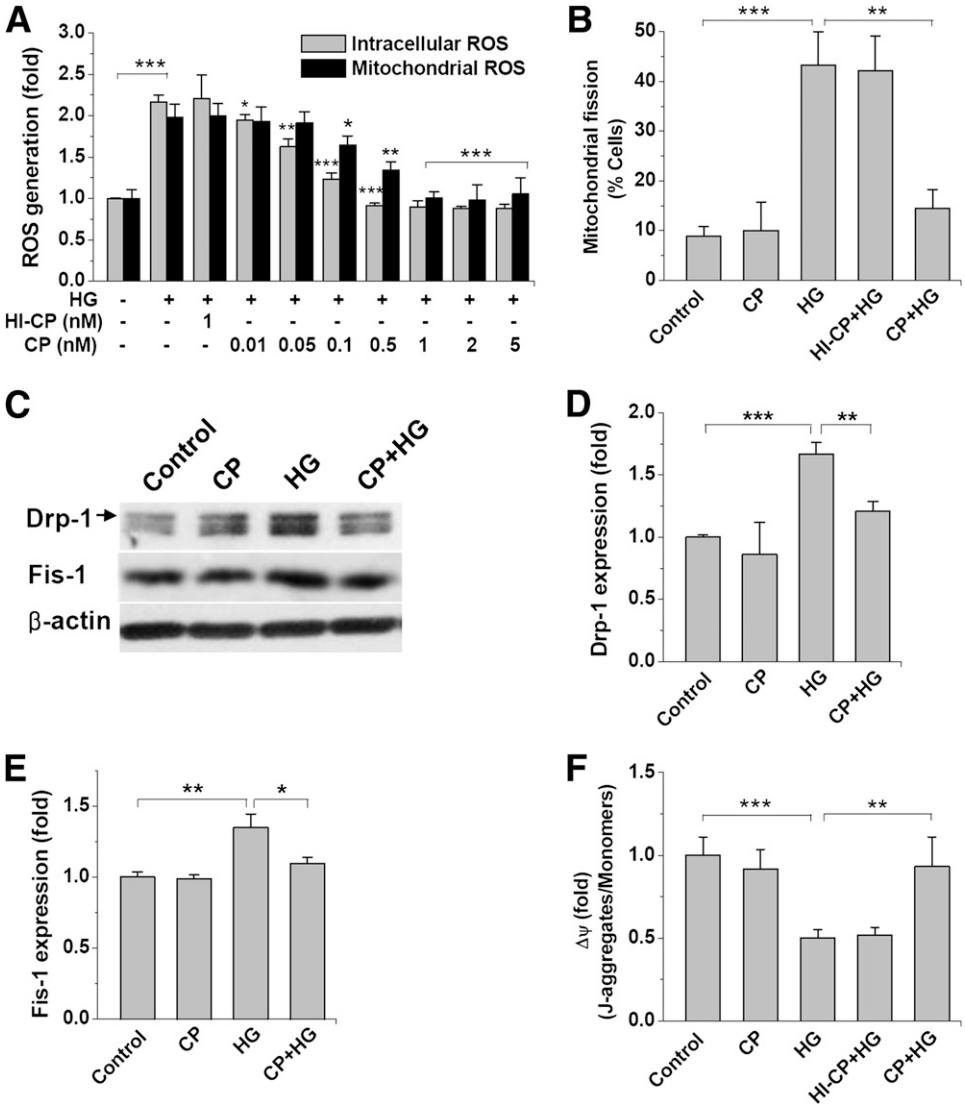

FIG. 3. C-peptide inhibits high glucose (HG)–induced ROS generation, mitochondrial fission, and $\Delta\Psi_m$ collapse. HUVECs were incubated with HG for 48 h in the presence of the indicated concentrations (*A*) or 1 nmol/L (*B–F*) of C-peptide (CP) or heat-inactivated C-peptide (HI-CP). ROS generation, mitochondrial fission, expression of Drp-1 and Fis-1, and $\Delta\Psi_m$ were determined as described in RESEARCH DESIGN AND METHODS. *A*: C-peptide inhibited HG-induced generation of intracellular and mitochondrial ROS in a dose-dependent manner. *$P < 0.05$, **$P < 0.01$, ***$P < 0.001$ compared with HG. *B*: C-peptide inhibited HG-induced mitochondrial fission. *C–E*: C-peptide inhibited HG-induced expression of Drp-1 (*D*) and Fis-1 (*E*). *C*: Western blot analysis of Drp-1 and Fis-1 expression. Expression levels were normalized to β-actin. *F*: C-peptide inhibited HG-induced $\Delta\Psi_m$ collapse. However, HI-CP had no inhibitory effect on HG-induced generation of intracellular and mitochondrial ROS (*A*), mitochondrial fission (*B*), and $\Delta\Psi_m$ collapse (*F*). *$P < 0.05$, **$P < 0.01$, ***$P < 0.001$. Data are expressed as mean ± SD of three independent experiments. Ctrl, control.

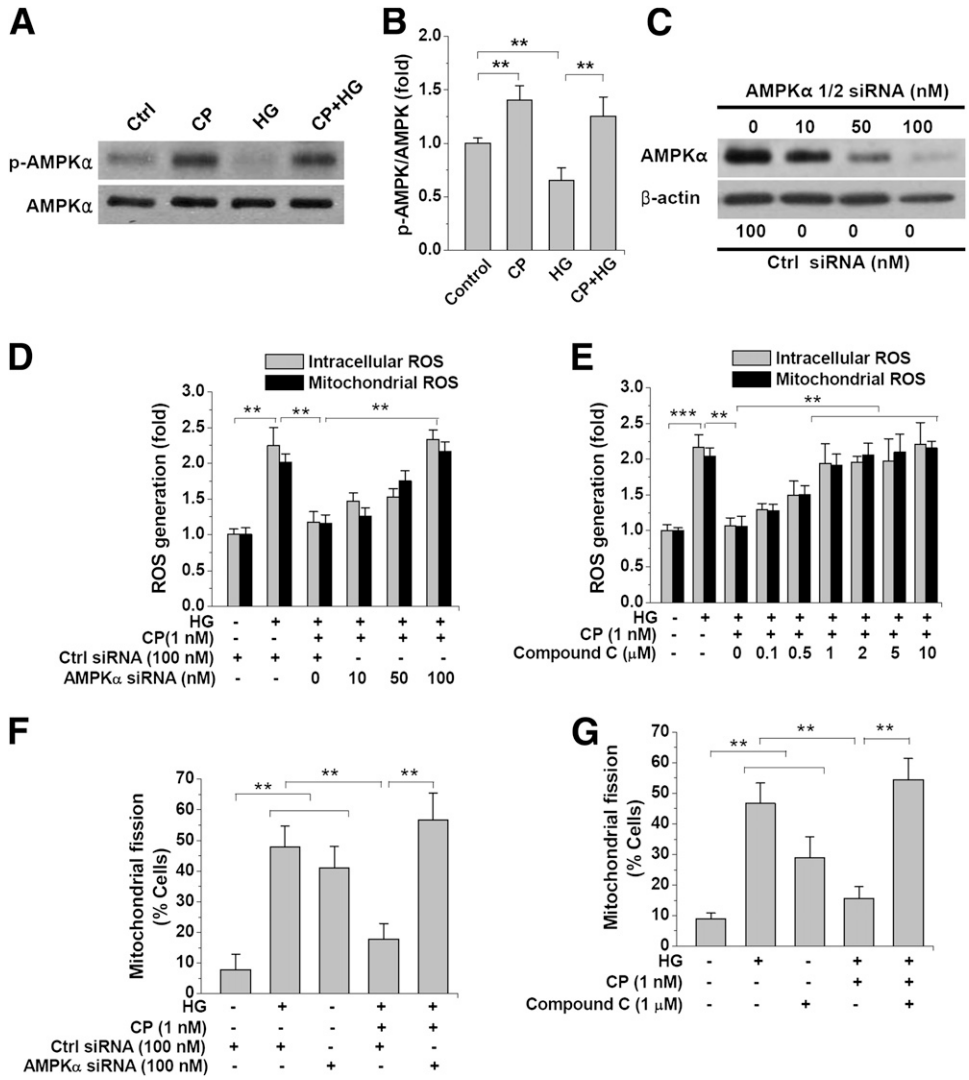

FIG. 4. Essential roles of AMPKα in C-peptide–mediated inhibition of high glucose (HG)–induced ROS generation, mitochondrial fission, and $\Delta\Psi_m$ collapse. HUVECs were transfected with the indicated concentrations of AMPKα1/2 siRNA or treated with the indicated concentrations of compound C and incubated with HG for 48 h. *A* and *B*: C-peptide (CP) activated AMPKα and rescued HG-induced AMPKα inhibition. *A*: A representative immunoblot. *B*: Quantification of AMPKα phosphorylation normalized to total AMPKα. *C*: siRNA concentration–dependent suppression of AMPKα expression. *D* and *E*: AMPKα siRNA (*D*) or compound C (*E*) inhibited C-peptide–mediated prevention of HG-induced intracellular and mitochondrial ROS production in a dose-dependent manner. *F* and *G*: Inhibition of HG-induced mitochondrial fission by AMPKα siRNA (*F*) or compound C (*G*). *H* and *I*: Inhibition of HG-induced $\Delta\Psi_m$ collapse by AMPKα siRNA (*H*) or compound C (*I*). *J*: Time course changes in the levels of NO by C-peptide. HUVECs were treated for the indicated times with 1 nmol/L C-peptide in the presence of control, 2 mmol/L L-NAME, or 1 μmol/L compound C. NO production was measured by confocal microscopy using DAF-FM diacetate staining. *K* and *L*: Possible role of C-peptide–induced NO production in AMPKα phosphorylation. HUVECs were treated with 1 nmol/L C-peptide, 1 nmol/L C-peptide with 2 mmol/L NO synthase inhibitor L-NAME, HG, or HG with 1 nmol/L NO donor *S*-nitroso-*N*-acetylpenicillamine (SNAP) for 48 h. Cell lysates were subjected to Western blot analysis to estimate AMPKα phosphorylation. *K*: A representative immunoblot. *L*: Quantification of AMPKα phosphorylation normalized to total AMPKα. *$P < 0.05$, **$P < 0.01$, and ***$P < 0.001$. Data are expressed as mean ± SD of three independent experiments. Ctrl, control.

AICAR and metformin mimic C-peptide–mediated prevention of high glucose–induced ROS generation, mitochondrial fission, and $\Delta\Psi_m$ collapse through AMPKα activation. AICAR and metformin each inhibited high glucose–induced generation of intracellular and mitochondrial ROS in a dose-dependent manner (Fig. 5*A* and *B*). AICAR and metformin also rescued high glucose–mediated inhibition of AMPKα as demonstrated by its phosphorylation at Thr^{172} (Fig. 5*C* and *D*). High glucose–stimulated mitochondrial fission was significantly inhibited by AICAR and metformin (Fig. 5*E*). Consistently, these AMPK activators inhibited high glucose–induced expression of Drp-1 and Fis-1 (data not shown). $\Delta\Psi_m$ collapse induced by high glucose was significantly reversed by AICAR and metformin (Fig. 5*F*). Additionally, the ROS scavenger Trolox significantly prevented high glucose–stimulated mitochondrial fission and $\Delta\Psi_m$ collapse (Fig. 5*E* and *F*). Thus, AICAR and metformin mimic C-peptide by preventing high glucose–induced mitochondrial fission and $\Delta\Psi_m$ collapse through AMPKα-mediated inhibition of intracellular and mitochondrial ROS generation.

C-peptide prevents endothelial cell apoptosis by AMPKα-mediated inhibition of ROS generation in hyperglycemia. We used the $DiOC_6$/PI double-staining assay (34) to exam whether C-peptide prevents high glucose–induced apoptosis by activating AMPK signaling. C-peptide prevented high glucose–induced apoptosis of endothelial cells (Fig. 6*A*). D-glucose induced the endothelial cell apoptosis in a dose-dependent manner, which was inhibited by C-peptide (Supplementary Fig. 1).

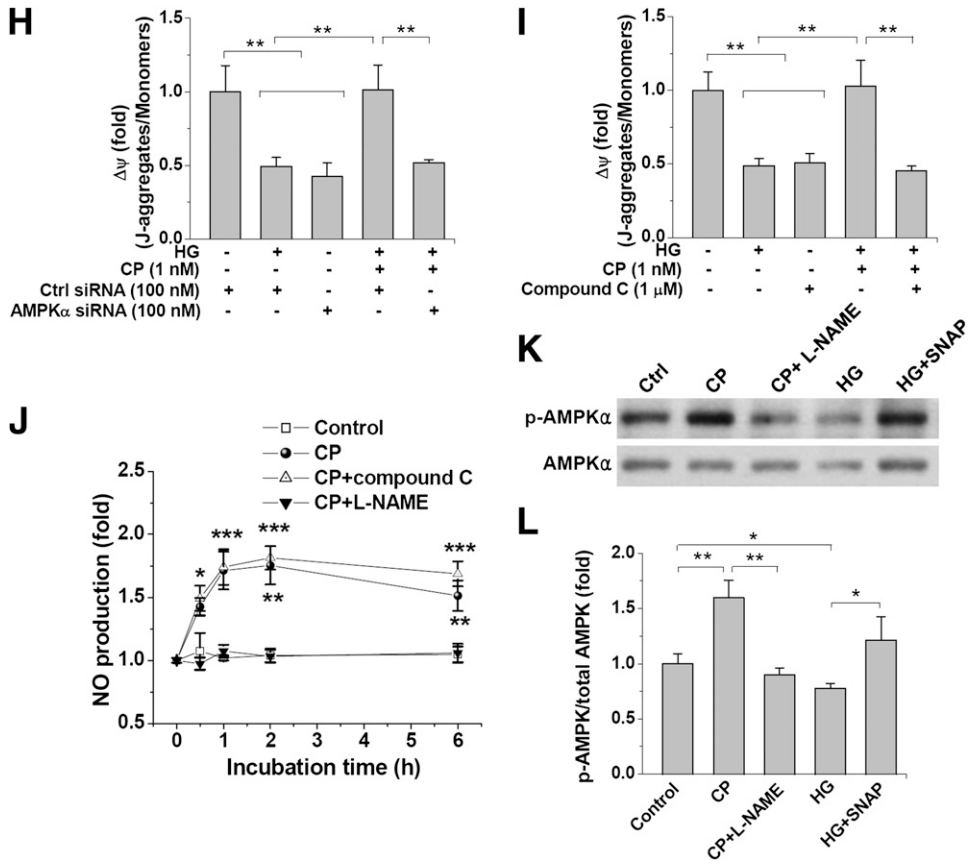

FIG. 4. Continued.

However, apoptotic cell death was neither activated by L-glucose nor inhibited by heat-inactivated C-peptide (Fig. 6*A*). Endothelial cell apoptosis was significantly inhibited by AMPK activators AICAR and metformin, the NADPH oxidase inhibitor apocynin, and the mitochondrial ROS scavenger mito-TEMPO (Fig. 6*A*). Thus, C-peptide prevents high glucose–induced endothelial cell apoptosis through activation of AMPK and inhibition of ROS generation. Moreover, inhibition of high glucose–induced apoptosis by Mdivi-1 (Fig. 6*A*) provides further evidence that Drp-1–dependent mitochondrial fission is important for high glucose–induced endothelial cell apoptosis.

The key role of AMPKα in C-peptide–mediated protection of endothelial cell death was further elucidated using AMPKα 1/2 siRNA and compound C (Fig. 6*B* and *C*). Transfection of AMPKα 1/2 siRNA or treatment with compound C significantly increased apoptosis (Fig. 6*B* and *C*). Moreover, C-peptide–mediated inhibition of high glucose–stimulated endothelial cell apoptosis was reversed by AMPKα 1/2 siRNA or compound C (Fig. 6*B* and *C*). Further, compound C reversed the C-peptide inhibition of dose-dependent high glucose–induced apoptosis (Supplementary Fig. 1). Thus, C-peptide protects endothelial cells from apoptosis by AMPKα-mediated inhibition of ROS generation and prevention of mitochondrial fission in hyperglycemia.

C-peptide promotes AMPKα activation and prevents ROS generation and mitochondrial fission in the aortas of streptozotocin diabetic mice. The role of AMPKα in C-peptide–mediated prevention of hyperglycemia-induced ROS generation and mitochondrial fission was further investigated in the aortas of streptozotocin diabetic mice. Five-week diabetic mice showed loss of body weight, increased rate of food and water consumption, and severe hyperglycemia (30.41 mmol/L) with glucosuria compared with nondiabetic controls (Supplementary Table 1). However, these parameters were not improved in diabetic mice supplemented with C-peptide. Serum C-peptide levels significantly decreased in untreated diabetic mice ($P < 0.001$) and were fully restored to the normal physiologic range (1.54 nmol/L) in diabetic mice supplemented with C-peptide using osmotic pumps (Supplementary Table 1).

Phosphorylation of AMPKα was decreased in the aortas of diabetic mice and was normalized by C-peptide replacement therapy (Fig. 7*A* and *B*). C-peptide supplementation also inhibited hyperglycemia-induced generation of intracellular ROS in aortic endothelial cells of diabetic mice (Fig. 7*C* and *D*). Furthermore, we assessed the preventive effect of C-peptide on mitochondrial fission. Hyperglycemia induced fragmentation and disorganization of mitochondria in the aortas of diabetic mice. C-peptide supplementation prevented hyperglycemia-stimulated mitochondrial fission (Fig. 7*E*). Consistently, we recently reported that C-peptide prevents hyperglycemia-induced apoptosis in the aortas of diabetic mice (17). Thus, consistent with our in vitro findings, C-peptide–mediated protection against hyperglycemia-induced apoptosis is due to AMPKα-dependent prevention of ROS generation and mitochondrial fission in aortic endothelium.

DISCUSSION

The development of vascular complications is associated with C-peptide deficiency in diabetes. We recently reported that C-peptide protects against ROS-mediated endothelial

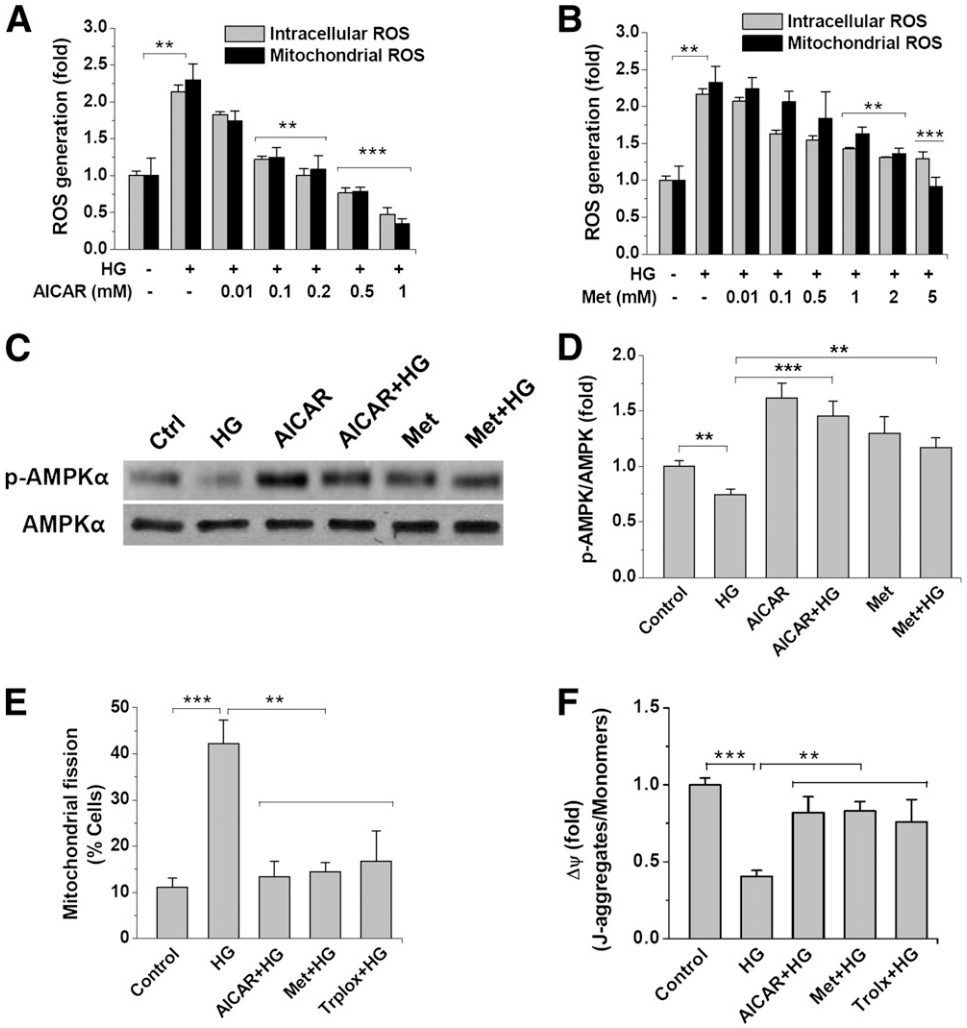

FIG. 5. AICAR and metformin inhibit high glucose (HG)–induced ROS generation, AMPKα dephosphorylation, mitochondrial fission, and $\Delta\Psi_m$ collapse. HUVECs were incubated with HG for 48 h in the presence of the indicated concentrations of AICAR and metformin (Met); 0.1 mmol/L AICAR and 2 mmol/L metformin were used for *C–F*. *A* and *B*: Inhibition of HG-induced intracellular and mitochondrial ROS generation by AICAR (*A*) and metformin (*B*) in a dose-dependent manner. **$P < 0.01$ and ***$P < 0.001$ compared with HG. *C* and *D*: AICAR and metformin rescued HG-induced inhibition of AMPKα. *C*: A representative immunoblot. *D*: Quantification of AMPKα phosphorylation normalized to total AMPKα. *E*: Inhibition of HG-induced mitochondrial fission by AICAR, metformin, and Trolox. *F*: Inhibition of HG-induced $\Delta\Psi_m$ collapse by AICAR, metformin, and Trolox. **$P < 0.01$ and ***$P < 0.001$. Data are expressed as mean ± SD of three independent experiments. Ctrl, control.

cell apoptosis; however, the mechanism by which C-peptide exerts ROS inhibition is not understood. In this article, we elucidated a new mechanism by which C-peptide prevents hyperglycemia-induced vasculopathy. As shown in Fig. 8, C-peptide inhibits high glucose–induced generation of intracellular and mitochondrial ROS through activation of AMPKα, which results in suppression of mitochondrial fission and $\Delta\Psi_m$ collapse and protects against endothelial cell apoptosis in response to hyperglycemia.

We targeted PKC-dependent NADPH oxidase and mitochondria because they are reported to be the two main sources of ROS generation in response to hyperglycemia in endothelial cells (12,14). Cytosolic NADPH oxidase and mitochondria played essential roles in amplifying intracellular ROS production in hyperglycemia. Inhibitors of the PKC-dependent NADPH oxidase pathway prevented high glucose–induced mitochondrial ROS generation, suggesting that cytosolic ROS facilitates mitochondrial ROS generation. Similarly, mitochondrial and intracellular ROS generation was inhibited by mito-TEMPO and Mdivi-1. Our results demonstrated the interregulation between cytosolic and mitochondrial ROS generation in response to high glucose in endothelial cells. Consistent with our findings, there was a recent report (36) of a vicious cycle in which mitochondrial superoxide stimulates cytosolic NADPH oxidase in a feed-forward fashion in response to angiotensin II in endothelial cells. Thus, it is likely that hyperglycemia triggers a positive feedback loop of intracellular ROS amplification in endothelial cells, in which cytosolic ROS production by PKC-dependent NADPH oxidase potentiates mitochondrial ROS increase and release, resulting in a further increase in cytosolic ROS.

We further investigated the potential link between ROS-dependent mitochondrial fission and apoptosis of endothelial cells in hyperglycemia. We found a prominent increase in mitochondrial fission upon treatment with high glucose in HUVECs. Blocking cytosolic ROS generation, inhibiting mitochondrial fission with Mdivi-1, or enhancing mitochondrial antioxidant activity with mito-TEMPO prevented mitochondrial fission. These results demonstrate that both

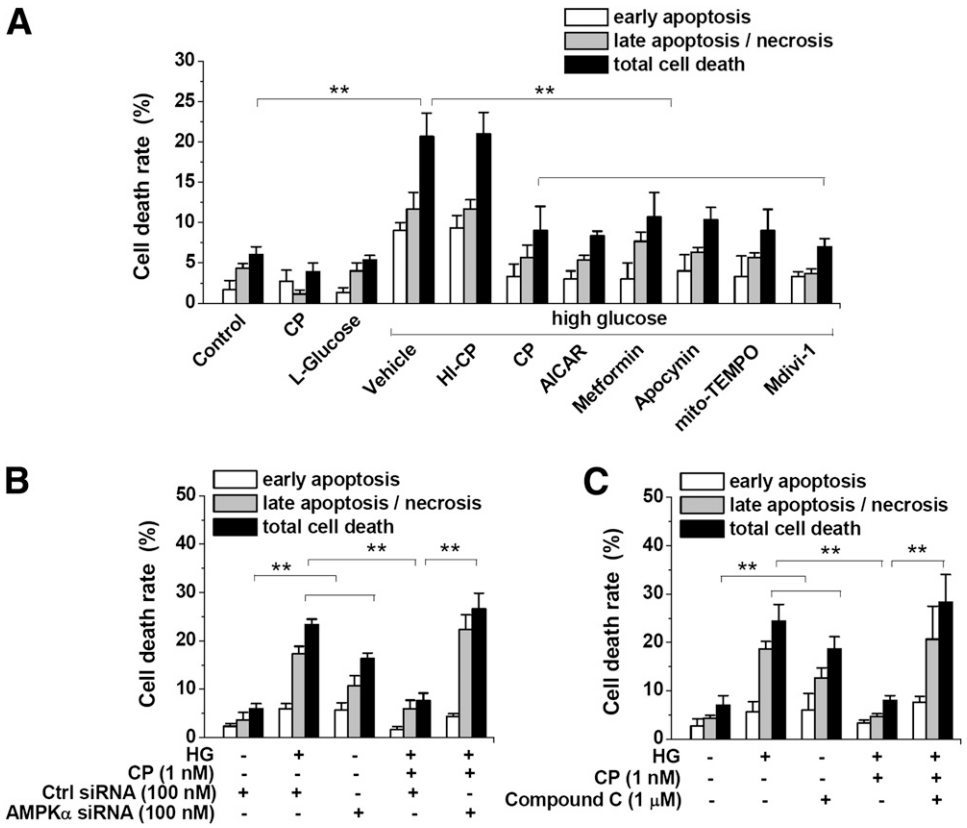

FIG. 6. Prevention of high glucose (HG)–induced apoptosis by various inhibitors and reversal of C-peptide effect by AMPK siRNA and compound C. HUVECs were incubated with HG for 72 h in the presence of inhibitors (*A* and *C*) or AMPKα siRNA (*B*). Early and late apoptotic cell death rates were determined as described in RESEARCH DESIGN AND METHODS. *A*: HG-induced apoptotic cell death was prevented by 1 nmol/L C-peptide, 0.1 mmol/L AICAR, 2 mmol/L metformin, 10 μmol/L apocynin, 10 μmol/L mito-TEMPO, and 10 μmol/L Mdivi-1. However, apoptotic cell death was neither activated by L-glucose nor inhibited by heat-inactivated C-peptide (HI-CP). *B* and *C*: AMPKα siRNA (*B*) and compound C (*C*) reversed C-peptide prevention of HG-induced apoptosis. **$P < 0.01$. Data are expressed as mean ± SD of three independent experiments. Ctrl, control.

cytosolic and mitochondrial ROS can enhance mitochondrial fission. We also found that ROS production and its downstream mitochondrial fission contributed to $\Delta\Psi_m$ collapse, which is considered to be an early stage of apoptosis (37). High glucose–induced $\Delta\Psi_m$ collapse was successfully prevented by blocking cytosolic and mitochondrial ROS or by inhibiting mitochondrial fission. Thus, intracellular ROS-mediated mitochondrial fission induces $\Delta\Psi_m$ collapse, which triggers apoptosis of endothelial cells during hyperglycemia (Fig. 8).

Our studies identify C-peptide–mediated activation of AMPKα as a novel mechanism that protects against hyperglycemia-induced vascular damage. AMPKα is considered to be an emerging therapeutic target for preventing diabetes complications (38–40). AMPK activation depends on phosphorylation of the α catalytic subunit at Thr^{172} and AMP binding to the γ subunit, whereas ATP promotes dephosphorylation of AMPK (41). Previous studies have shown that AMPKα is dephosphorylated and has diminished activity in diabetes (31,32,42). In this article, we demonstrated that C-peptide activates phosphorylation of AMPKα. Further, we showed that high glucose–stimulated dephosphorylation of AMPKα was reversed by C-peptide in HUVECs. AMPKα siRNA or the AMPK inhibitor, compound C, also inhibited C-peptide–mediated prevention of high glucose–induced apoptosis of endothelial cells by inhibiting ROS generation, mitochondrial fission, and $\Delta\Psi_m$ collapse. Additionally, the beneficial role of C-peptide against intracellular ROS amplification and mitochondrial fission through AMPKα activation was elucidated in the aortas of streptozotocin diabetic mice supplemented with C-peptide. Furthermore, AICAR and metformin mimicked the preventive effect of C-peptide on high glucose–induced ROS generation, AMPK dephosphorylation, mitochondrial fission, $\Delta\Psi_m$ collapse, and endothelial cell apoptosis. Thus, it is likely that AMPKα is essential for C-peptide–mediated prevention of hyperglycemia-induced vascular complications.

It would be interesting to elucidate the mechanism by which C-peptide activates AMPKα. It is reported that C-peptide stimulates endothelial NO synthase (43). NO can act as an endogenous activator of AMPK in vascular endothelial cells (44). In the current study, C-peptide elevated the level of intracellular NO. Compound C had no significant effect on the C-peptide–induced formation of NO, whereas L-NAME inhibited the NO formation, indicating that AMPK is not involved in the C-peptide–stimulated NO production. C-peptide activated AMPKα at 48 h, and the activation was significantly inhibited by L-NAME. Additionally, *S*-nitroso-*N*-acetylpenicillamine recovered high glucose–induced AMPKα dephosphorylation. Thus, it is possible to propose that NO production can contribute to the C-peptide stimulation of AMPKα phosphorylation in endothelial cells; however, it is necessary to elucidate the mechanism by which early NO formation can induce the late activation of AMPKα in response to C-peptide.

The major upstream kinase activating AMPK is the tumor suppressor liver kinase B1 (LKB1), which is essential

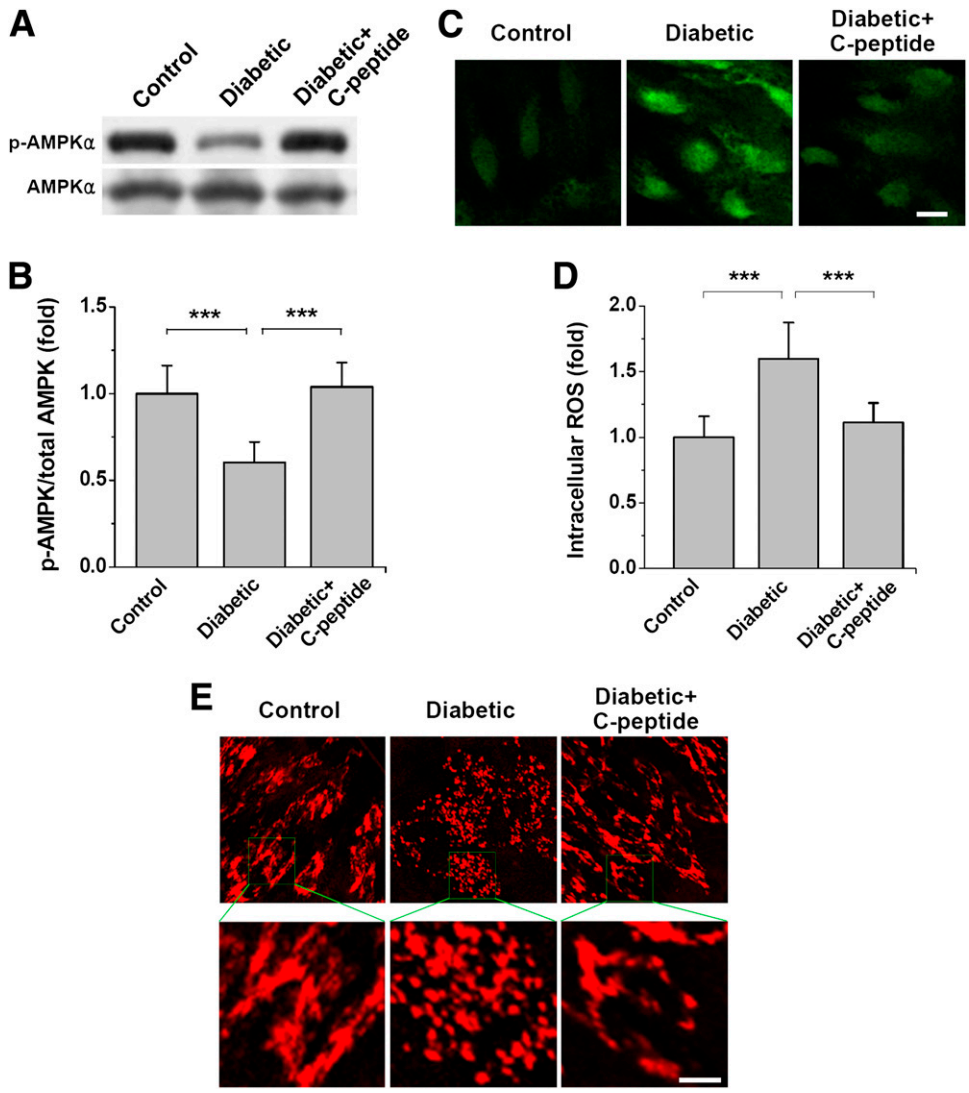

FIG. 7. C-peptide replacement therapy inhibits hyperglycemia-induced AMPKα dephosphorylation, intracellular ROS generation, and mitochondrial fission in diabetic mice. Streptozotocin diabetic mice were subcutaneously implanted for 4 weeks with Alzet mini-osmotic pumps containing C-peptide. Aorta from control (n = 8), diabetic (n = 8), and diabetic plus C-peptide (n = 7) groups of mice were dissected and cut longitudinally to open the endothelium. AMPKα phosphorylation, intracellular ROS generation, and mitochondrial fission were immediately measured as described in RESEARCH DESIGN AND METHODS. *A* and *B*: Dephosphorylation of AMPKα at Thr^{172} was induced by hyperglycemia in diabetic mice and was normalized in C-peptide–supplemented diabetic mice (n = 7). *A*: A representative immunoblot. *B*: Densitometric quantification of AMPKα activation normalized to total AMPKα. *C* and *D*: Generation of intracellular ROS was increased by hyperglycemia in the aortic endothelium of diabetic mice (n = 8) and was normalized in C-peptide–supplemented diabetic mice (n = 7). *C*: Measurement of intracellular ROS levels using H_2DCFDA; bar, 20 μm. *D*: Quantification of intracellular ROS compared with control. *E*: Mitochondrial fission was increased by hyperglycemia in diabetic mice (n = 8) and was normalized in C-peptide–supplemented mice (n = 7); bar, 5 μm. ***$P < 0.001$.

for the AMPK activation by AICAR (45). In our study, AICAR mimicked C-peptide by preventing high glucose–induced ROS generation, mitochondrial fission, $\Delta\Psi_m$ collapse, and cell death, suggesting that C-peptide activation of AMPKα might involve LKB1. Additionally, protein phosphatase 2C might be involved in the C-peptide activation of AMPK, since increase in intracellular AMP levels promotes AMPKα phosphorylation by inhibiting its dephosphorylation by the protein phosphatase 2C (46). However, Ca^{2+}/calmodulin-dependent protein kinase kinase β is unlikely involved in the C-peptide activation of AMPK because C-peptide has no effect on the level of intracellular Ca^{2+} in endothelial cells (17).

In conclusion, our data indicate that cross-talk between PKC-dependent NADPH oxidase and mitochondrial ROS generation results in a positive feedback loop that amplifies intracellular ROS production in endothelial cells. Amplification of intracellular ROS generation mediates mitochondrial fission, which then leads to ΔΨm collapse and apoptosis of endothelial cells in diabetes. Importantly, our data support C-peptide supplementation as a new therapeutic strategy for preventing diabetic vascular complications. C-peptide–mediated activation of AMPKα inhibited hyperglycemia-induced intracellular ROS production, mitochondrial fission, and endothelial cell apoptosis. Supplementation with C-peptide may offer increased benefit beyond the limits of currently available pharmacological agents, such as AICAR and metformin. Thus, C-peptide supplementation should be tested in combination with insulin therapy as a new strategy for preventing vascular complications in type 1 diabetes and late-stage type 2 diabetes.

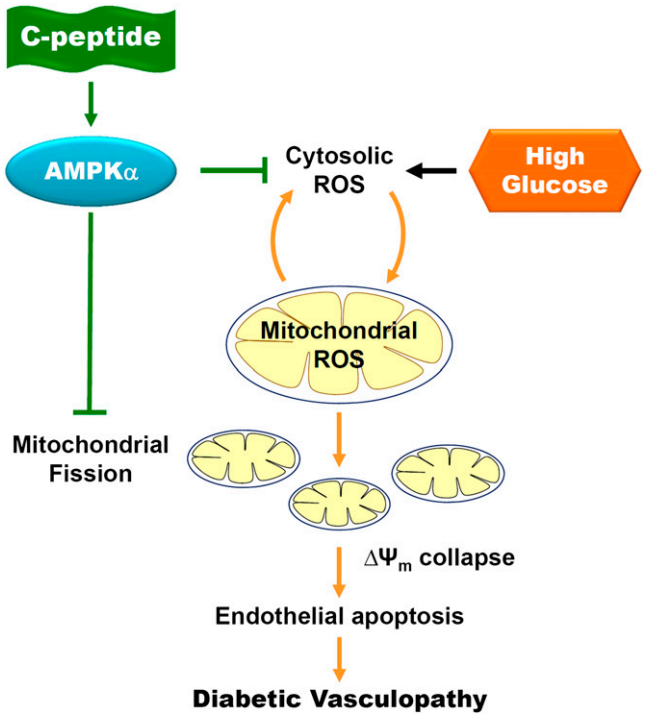

FIG. 8. Schematic model depicting the role of C-peptide in the regulation of hyperglycemia-induced vasculopathy through an AMPKα-dependent mechanism.

ACKNOWLEDGMENTS

This work was supported in part by Korea Research Foundation of Korea grants (2008-05943 and 2013-008193) and by the Ministry of Health and Welfare through the National R&D Program for Cancer Control (1020420).

No potential conflicts of interest relevant to this article were reported.

M.P.B. researched data and wrote the manuscript. Y.-C.L. researched data. Y.-M.K. contributed to discussion. K.-S.H. designed and supervised experiments and edited the manuscript. K.-S.H. is the guarantor of this work and, as such, had full access to all the data in the study and takes responsibility for the integrity of the data and the accuracy of the data analysis.

REFERENCES

1. Wahren J, Kallas A, Sima AA. The clinical potential of C-peptide replacement in type 1 diabetes. Diabetes 2012;61:761–772
2. Massi-Benedetti M, Orsini-Federici M. Treatment of type 2 diabetes with combined therapy: what are the pros and cons? Diabetes Care 2008;31 (Suppl. 2):S131–S135
3. Heine RJ, Diamant M, Mbanya JC, Nathan DM. Management of hyperglycaemia in type 2 diabetes: the end of recurrent failure? BMJ 2006;333: 1200–1204
4. McCarthy MI. Genomics, type 2 diabetes, and obesity. N Engl J Med 2010; 363:2339–2350
5. Ido Y, Vindigni A, Chang K, et al. Prevention of vascular and neural dysfunction in diabetic rats by C-peptide. Science 1997;277:563–566
6. Johansson BL, Borg K, Fernqvist-Forbes E, Kernell A, Odergren T, Wahren J. Beneficial effects of C-peptide on incipient nephropathy and neuropathy in patients with type 1 diabetes mellitus. Diabet Med 2000;17:181–189
7. Vejandla H, Hollander JM, Kothur A, Brock RW. C-Peptide reduces mitochondrial superoxide generation by restoring complex I activity in high glucose-exposed renal microvascular endothelial cells. ISRN Endocrinol 2012;2012:162802
8. Scalia R, Coyle KM, Levine BJ, Booth G, Lefer AM. C-peptide inhibits leukocyte-endothelium interaction in the microcirculation during acute endothelial dysfunction. FASEB J 2000;14:2357–2364
9. Luppi P, Cifarelli V, Tse H, Piganelli J, Trucco M. Human C-peptide antagonises high glucose-induced endothelial dysfunction through the nuclear factor-kappaB pathway. Diabetologia 2008;51:1534–1543
10. Cifarelli V, Luppi P, Tse HM, He J, Piganelli J, Trucco M. Human proinsulin C-peptide reduces high glucose-induced proliferation and NF-kappaB activation in vascular smooth muscle cells. Atherosclerosis 2008;201:248–257
11. Mughal RS, Scragg JL, Lister P, et al. Cellular mechanisms by which proinsulin C-peptide prevents insulin-induced neointima formation in human saphenous vein. Diabetologia 2010;53:1761–1771
12. Brownlee M. Biochemistry and molecular cell biology of diabetic complications. Nature 2001;414:813–820
13. Touyz RM, Briones AM. Reactive oxygen species and vascular biology: implications in human hypertension. Hypertens Res 2011;34:5–14
14. Inoguchi T, Li P, Umeda F, et al. High glucose level and free fatty acid stimulate reactive oxygen species production through protein kinase C–dependent activation of NAD(P)H oxidase in cultured vascular cells. Diabetes 2000;49:1939–1945
15. Quagliaro L, Piconi L, Assaloni R, Martinelli L, Motz E, Ceriello A. Intermittent high glucose enhances apoptosis related to oxidative stress in human umbilical vein endothelial cells: the role of protein kinase C and NAD(P)H-oxidase activation. Diabetes 2003;52:2795–2804
16. Baumgartner-Parzer SM, Wagner L, Pettermann M, Grillari J, Gessl A, Waldhäusl W. High-glucose–triggered apoptosis in cultured endothelial cells. Diabetes 1995;44:1323–1327
17. Bhatt MP, Lim YC, Hwang J, Na S, Kim YM, Ha KS. C-peptide prevents hyperglycemia-induced endothelial apoptosis through inhibition of reactive oxygen species-mediated transglutaminase 2 activation. Diabetes 2013;62:243–253
18. Giacco F, Brownlee M. Oxidative stress and diabetic complications. Circ Res 2010;107:1058–1070
19. Nishikawa T, Edelstein D, Du XL, et al. Normalizing mitochondrial superoxide production blocks three pathways of hyperglycaemic damage. Nature 2000;404:787–790
20. Shenouda SM, Widlansky ME, Chen K, et al. Altered mitochondrial dynamics contributes to endothelial dysfunction in diabetes mellitus. Circulation 2011;124:444–453
21. Yu T, Robotham JL, Yoon Y. Increased production of reactive oxygen species in hyperglycemic conditions requires dynamic change of mitochondrial morphology. Proc Natl Acad Sci USA 2006;103:2653–2658
22. Wang S, Song P, Zou MH. AMP-activated protein kinase, stress responses and cardiovascular diseases. Clin Sci (Lond) 2012;122:555–573
23. Zhang BB, Zhou G, Li C. AMPK: an emerging drug target for diabetes and the metabolic syndrome. Cell Metab 2009;9:407–416
24. Ceolotto G, Gallo A, Papparella I, et al. Rosiglitazone reduces glucose-induced oxidative stress mediated by NAD(P)H oxidase via AMPK-dependent mechanism. Arterioscler Thromb Vasc Biol 2007;27:2627–2633
25. Davis BJ, Xie Z, Viollet B, Zou MH. Activation of the AMP-activated kinase by antidiabetes drug metformin stimulates nitric oxide synthesis in vivo by promoting the association of heat shock protein 90 and endothelial nitric oxide synthase. Diabetes 2006;55:496–505
26. Kim JE, Song SE, Kim YW, et al. Adiponectin inhibits palmitate-induced apoptosis through suppression of reactive oxygen species in endothelial cells: involvement of cAMP/protein kinase A and AMP-activated protein kinase. J Endocrinol 2010;207:35–44
27. Ido Y, Carling D, Ruderman N. Hyperglycemia-induced apoptosis in human umbilical vein endothelial cells: inhibition by the AMP-activated protein kinase activation. Diabetes 2002;51:159–167
28. Kukidome D, Nishikawa T, Sonoda K, et al. Activation of AMP-activated protein kinase reduces hyperglycemia-induced mitochondrial reactive oxygen species production and promotes mitochondrial biogenesis in human umbilical vein endothelial cells. Diabetes 2006;55:120–127
29. Wang S, Zhang M, Liang B, et al. AMPKalpha2 deletion causes aberrant expression and activation of NAD(P)H oxidase and consequent endothelial dysfunction in vivo: role of 26S proteasomes. Circ Res 2010;106:1117–1128
30. Colombo SL, Moncada S. AMPKalpha1 regulates the antioxidant status of vascular endothelial cells. Biochem J 2009;421:163–169
31. Wang XR, Zhang MW, Chen DD, Zhang Y, Chen AF. AMP-activated protein kinase rescues the angiogenic functions of endothelial progenitor cells via manganese superoxide dismutase induction in type 1 diabetes. Am J Physiol Endocrinol Metab 2011;300:E1135–E1145
32. Garcia-Haro L, Garcia-Gimeno MA, Neumann D, Beullens M, Bollen M, Sanz P. The PP1-R6 protein phosphatase holoenzyme is involved in the glucose-induced dephosphorylation and inactivation of AMP-activated protein kinase, a key regulator of insulin secretion, in MIN6 beta cells. FASEB J 2010;24:5080–5091
33. Yoo JO, Lim YC, Kim YM, Ha KS. Transglutaminase 2 promotes both caspase-dependent and caspase-independent apoptotic cell death via the

calpain/Bax protein signaling pathway. J Biol Chem 2012;287:14377–14388
34. Yoo JO, Lim YC, Kim YM, Ha KS. Differential cytotoxic responses to low- and high-dose photodynamic therapy in human gastric and bladder cancer cells. J Cell Biochem 2011;112:3061–3071
35. Cassidy-Stone A, Chipuk JE, Ingerman E, et al. Chemical inhibition of the mitochondrial division dynamin reveals its role in Bax/Bak-dependent mitochondrial outer membrane permeabilization. Dev Cell 2008;14:193–204
36. Dikalova AE, Bikineyeva AT, Budzyn K, et al. Therapeutic targeting of mitochondrial superoxide in hypertension. Circ Res 2010;107:106–116
37. Giedt RJ, Yang C, Zweier JL, Matzavinos A, Alevriadou BR. Mitochondrial fission in endothelial cells after simulated ischemia/reperfusion: role of nitric oxide and reactive oxygen species. Free Radic Biol Med 2012;52:348–356
38. Zang M, Xu S, Maitland-Toolan KA, et al. Polyphenols stimulate AMP-activated protein kinase, lower lipids, and inhibit accelerated atherosclerosis in diabetic LDL receptor-deficient mice. Diabetes 2006;55:2180–2191
39. Viollet B, Lantier L, Devin-Leclerc J, et al. Targeting the AMPK pathway for the treatment of type 2 diabetes. Front Biosci 2009;14:3380–3400
40. Cool B, Zinker B, Chiou W, et al. Identification and characterization of a small molecule AMPK activator that treats key components of type 2 diabetes and the metabolic syndrome. Cell Metab 2006;3:403–416
41. Oakhill JS, Steel R, Chen ZP, et al. AMPK is a direct adenylate charge-regulated protein kinase. Science 2011;332:1433–1435
42. Eid AA, Ford BM, Block K, et al. AMP-activated protein kinase (AMPK) negatively regulates Nox4-dependent activation of p53 and epithelial cell apoptosis in diabetes. J Biol Chem 2010;285:37503–37512
43. Wallerath T, Kunt T, Forst T, et al. Stimulation of endothelial nitric oxide synthase by proinsulin C-peptide. Nitric Oxide 2003;9:95–102
44. Zhang J, Xie Z, Dong Y, Wang S, Liu C, Zou MH. Identification of nitric oxide as an endogenous activator of the AMP-activated protein kinase in vascular endothelial cells. J Biol Chem 2008;283:27452–27461
45. Fisslthaler B, Fleming I. Activation and signaling by the AMP-activated protein kinase in endothelial cells. Circ Res 2009;105:114–127
46. Sanders MJ, Grondin PO, Hegarty BD, Snowden MA, Carling D. Investigating the mechanism for AMP activation of the AMP-activated protein kinase cascade. Biochem J 2007;403:139–148